Amyloid burden, cerebrovascular disease, brain atrophy, and cognition in cognitively impaired patients

Byoung Seok Ye

Department of medicine

The Graduate School, Yonsei University

Amyloid burden, cerebrovascular disease, brain atrophy, and cognition in cognitively impaired patients

Directed by Professor Young H. Sohn

Doctoral Dissertation
submitted to the Department of medicine,
the Graduate School of Yonsei University
in partial fulfillment of the requirements for the degree of
Doctor of Philosophy

Byoung Seok Ye

December 2014

This certifies that the Doctoral Dissertation
of Byoung Seok Ye is approved.

Thesis Supervisor : Young H. Sohn

Thesis Committee Member#1 : Duk L. Na

Thesis Committee Member#2 : Phil Hyu Lee

Thesis Committee Member#3: Jong Du Lee

Thesis Committee Member#4: Seung-Koo Lee

The Graduate School
Yonsei University

December 2014

ACKNOWLEDGEMENTS

It is an honor for me to thank my supervisor, Professor Young Ho Sohn, whose encouragement, guidance, and support from the initial to the final level enabled me to write this thesis.

I am grateful that Professor Sang Won Seo and Professor Duk L. Na have overseen the planning of this thesis and have acted as consultants and meticulous first readers. They also gave me their guidance, valuable feedback, and comments.

My sincere thanks go to Professor Phil Hyu Lee whose perspective critism and kind encouragement helped bring the completion of this thesis, Professor Jong Du Lee who has generously proofread every page of this work several times offering detailed and invaluable comments, and to Professor Seung-Koo Lee who has enormously contributed to improving this manuscript.

Lastly, I want to offer my kind regards and blessings to all those who have supported me, including my family, especially my wife, Jieun Lee, and my daughter, Seoyoon Ye. I love you.

December 2014

<TABLE OF CONTENTS>

LIST OF FIGURES

LIST OF TABLES

ABSTRACT

Amyloid burden, cerebrovascular disease, brain atrophy, and cognition in cognitively impaired patients

Byoung Seok Ye

Department of Medicine,
The Graduate School, Yonsei University

(Directed by Professor Young H. Sohn)

Background: We investigated the independent effects of Alzheimer's disease (AD) and cerebrovascular disease (CVD) pathologies on brain structural changes and cognition.

Methods: Amyloid burden (Pittsburgh compound B (PiB) retention ratio), CVD markers (volume of white matter hyperintensities (WMH) and number of lacunae), and structural changes (cortical thickness and hippocampal shape) were measured in 251 cognitively impaired patients. Path analyses were utilized to assess the effects of these markers on cognition.

Results: PiB retention ratio was associated with hippocampal atrophy, which was associated with memory impairment. WMH were associated with frontal thinning, which was associated with executive and memory dysfunctions. PiB retention ratio and lacunae were also associated with memory and executive dysfunction without the mediation of hippocampal or frontal atrophy.

Conclusions: Our results suggest that the impacts of AD and CVD pathologies on cognition are mediated by specific brain regions.

Key words : Cognition; Amyloid; Pittsburgh Compound B; Atrophy; Cortical thickness; Hippocampus; Path analysis; Cerebrovascular disease

Amyloid burden, cerebrovascular disease, brain atrophy, and cognition in cognitively impaired patients

Byoung Seok Ye

Department of Medicine,
The Graduate School, Yonsei University

(Directed by Professor Young H. Sohn)

I. INTRODUCTION

Alzheimer's disease (AD) and subcortical vascular dementia (SVaD) are common types of dementia in the elderly[1,2]. AD results from an imbalance in amyloid beta (Aβ) production and clearance, which lead to amyloid plaque accumulation. SVaD is characterized by extensive cerebrovascular disease (CVD) magnetic resonance imaging (MRI) markers, including white matter hyperintensities (WMH) and lacunae[3]. Postmortem studies have shown that AD and SVaD pathologies frequently co-occur[4,5]. There is also increasing evidence that AD and CVD pathologies contribute independently to impairment of specific cognitive domains[6,7]. Pathological and Pittsburgh compound B (PiB) positron emission tomography (PET) studies have shown that AD pathology is associated with memory dysfunction, while CVD pathology affects multiple cognitive domains, including memory and executive function[7-9], although controversy still remains regarding these conclusions[10].

Previous studies of AD patients have shown that amyloid burden is associated with medial temporal cortical atrophy, including that of the hippocampus[11]. Also, recent studies have shown that WMH might affect brain atrophy, although those WMH were located in subcortical regions[12,13]. However, these studies did not evaluate the independent effects of amyloid burden and CVD on brain atrophy. Further, no studies have evaluated the relationship among amyloid, CVD, brain atrophy, and cognitive impairments. Brain atrophy associated with amyloid burden[14] or

WMH[12,13,15] was reported to correlate strongly with cognitive impairment[11,12,15]. Some researchers have also proposed that cognitive impairment may be more highly correlated with cortical atrophy than with amyloid burden[11] or WMH[16], implying that cortical atrophy may be the final common pathway of AD and SVaD. Therefore, it is possible that amyloid burden and CVD markers might drive cognitive impairment via the mediation of cortical or hippocampal atrophy. Alternatively, amyloid burden and CVD markers might affect cognitive impairment without the mediation of cortical or hippocampal atrophy. Actually, some studies have shown that the significant relationship between amyloid burden or CVD markers and cognitive impairment remains after controlling for cortical or hippocampal atrophy[17,18].

In this study, we investigated a large sample of patients with cognitive impairments who underwent PiB-PET, MRI, and detailed neuropsychological testing. The first goal was to evaluate the independent effects of amyloid burden evaluated through PiB-PET, and CVD, measured by the volume of WMH and number of lacunae, on the topography of brain atrophy, including hippocampal deformities or cortical thinning. The following hypotheses concerning the relationships among amyloid burden, CVD, brain atrophy, and cognitive impairment using path analyses were also tested. First, amyloid burden or CVD may drive memory dysfunction via hippocampal atrophy or frontal thinning. Second, amyloid burden or CVD might drive executive dysfunction via frontal thinning.

II. MATERIALS AND METHODS

1. Participants

We prospectively recruited 251 patients with cognitive impairment who had undergone PiB PET and structural brain MRI during the period from July 2007 to July 2011. We included 45 patients with amnestic mild cognitive impairment (aMCI), 69 with probable AD dementia, 67 with subcortical vascular MCI (svMCI), and 70 with subcortical vascular dementia (SVaD) who had all been clinically diagnosed at Samsung Medical Center. Probable AD dementia patients met criteria proposed by the

National Institute of Neurological and Communicative Disorders and Stroke and the AD and Related Disorders Association[19]. Patients with SVaD met the diagnostic criteria for vascular dementia as determined by the Diagnostic and Statistical Manual of Mental Disorders–Fourth Edition (DSM-IV) and also fulfilled the imaging criteria for SVaD as proposed by Erkinjuntti et al.[20]. The aMCI and svMCI patients met Petersen's criteria for MCI with modifications, as previously described[21]. All svMCI and SVaD patients had severe WMH defined as a cap or band (periventrivular WMH, PWMH) ≥ 10 mm and deep white-matter lesions (deep WMH, DWMH) ≥ 25 mm, as modified from Fazekas' MRI ischemia criteria[22]. All aMCI and AD were classified as having minimal (PWMH < 5mm and DWMH < 10mm) or moderate (between minimal and severe grades) WMH. Detailed criteria for aMCI and svMCI are described in online data supplement 1. Patients with aMCI or AD were considered to have AD-related cognitive impairment (ADCI), while those with svMCI or SVaD were considered to have subcortical vascular cognitive impairment (SVCI). Patients with territorial infarctions and those with WMH due to radiation injury, multiple sclerosis, vasculitis, or leukodystrophy were excluded.

Each patient underwent a clinical interview; neurological examinations; a battery of neuropsychological tests; laboratory tests including a complete blood count, blood chemistry, vitamin B12/folate measurement, syphilis serology, thyroid function, apolipoprotein E (*APOE*) genotyping, and PiB PET scan.

Written informed consent was obtained from every patient. The institutional review board of Samsung Medical Center approved the study protocol. Participant characteristics are summarized in Table 1.

Table 1. Demographics, clinical characteristics, and MRI markers in study participants

Group	Total	ADCI			SVCI		
		Subtotal	aMCI	AD	Subtotal	svMCI	SVaD
Number	251	114	45	69	137	67	70
Demographics							
Age, yr	72.1 (8.1)	70.0 (8.9)*	70.0 (8.0)	70.0 (9.5)	73.8 (6.9)	73.7 (6.7)	74.0 (7.1)
Sex, female, n (%)	146 (58.2)	64 (56.1)	20 (44.4)	44 (63.8)	82 (59.9)	41 (61.2)	41 (58.6)
Education, yr	10.1 (5.3)	11.3 (5.2)[*]	12.5 (4.6)	10.6 (5.5)	9.0 (5.2)	9.4 (5.4)	8.7 (5.0)
Cardiovascular risk factors, n (%)							
Hypertension	157 (62.5)	52 (45.6)[*]	17 (37.8)	35 (50.7)	105 (76.6)	50 (74.6)	55 (78.6)
Diabetes mellitus	51 (20.3)	16 (14.0)[*]	5 (11.1)	11 (15.9)	35 (25.5)	17 (25.4)	18 (25.7)
Hyperlipidemia	73 (29.1)	26 (22.8)[*]	10 (22.2)	16 (23.2)	47 (34.3)	20 (29.9)	27 (38.6)
Heart disease	37 (14.7)	12 (10.5)	7 (15.6)	5 (7.2)	25 (18.2)	17 (25.4)	8 (11.4)
APOE genotype, n (%)[†]							
ε2 allele carrier	25 (10.2)	8 (7.1)[*]	3 (6.7)	5 (7.5)	17 (12.7)	10 (14.9)	7 (10.4)
ε4 allele carrier	88 (35.8)	53 (47.3)[*]	19 (42.2)	34 (50.7)	35 (26.1)	15 (22.4)	20 (29.9)

Group	Total	ADCI			SVCI		
		Subtotal	aMCI	AD	Subtotal	svMCI	SVaD
Small vessel MRI markers							
WMH volume, ml	23.5 (22.3)	4.8 (6.7)*	3.1 (3.1)	5.9 (8.1)	39.0 (18.3)	34.9 (17.8)	43.0 (18.1)
Lacunae, n	6.8 (11.8)	0.5 (1.6)*	0.5 (2.1)	0.4 (1.0)	11.9 (13.9)	7.5 (8.4)	16.1 (16.6)
Global PiB global retention ratio	1.8 (0.5)	2.0 (0.5)*	1.8 (0.5)	2.2 (0.4)	1.5 (0.4)	1.5 (0.4)	1.5 (0.5)
PiB-positive patients, n (%)‡	134 (53.4)	90 (78.9)	28 (62.2)	62 (89.9)	44 (32.1)	21 (31.3)	23 (32.9)
Intracranial volume, ml	1362.2 (126.3)	1353.2 (129.4)	1377.5 (119.8)	1337.4 (133.7)	1369.6 (123.7)	1356.5 (104.7)	1382.1 (139.2)
Mean frontal thickness, mm	2.9 (0.2)	2.9 (0.2)*	3.0 (0.1)	2.9 (0.3)	2.8 (0.2)	2.9 (0.2)	2.7 (0.3)
Mean parietal thickness, mm	2.7 (0.3)	2.7 (0.3)	2.8 (0.2)	2.6 (0.3)	2.7 (0.2)	2.7 (0.2)	2.6 (0.2)
Mean temporal thickness, mm	2.9 (0.3)	3.0 (0.3)	3.1 (0.2)	2.9 (0.3)	2.9 (0.3)	3.0 (0.2)	2.8 (0.3)
Hippocampal volume, ml	2.4 (0.5)	2.3 (0.5)*	2.6 (0.5)	2.1 (0.4)	2.5 (0.5)	2.5 (0.5)	2.4 (0.4)
Executive score	24.2 (11.6)	26.6 (11.9)*	33.7 (9.9)	20.5 (10.4)	23.1 (10.6)	29.3 (8.5)	15.8 (8.7)
Memory score	41.8 (21.6)	36.0 (18.5)*	49.9 (17.0)	25.5 (11.8)	47.0 (22.7)	61.0 (19.5)	33.3 (16.2)
MMSE	22.7 (5.1)	22.0 (5.2)*	26.1 (2.5)	19.2 (4.7)	23.3 (4.9)	26.2 (3.0)	20.6 (4.8)

Abbreviations: aMCI, amnestic Mild Cognitive Impairment; AD, Alzheimer's disease; ADCI, Alzheimer's disease-related cognitive impairment; SVCI, subcortical vascular cognitive impairment; svMCI, subcortical vascular mild cognitive impairment; SVaD, subcortical vascular dementia; APOE, apolipoprotein E; WMH, white matter hyperintensities; PiB, Pittsburgh compound B; MMSE, mini-mental status examination.

[*] p value < 0.05 in the Chi-square test or independent t-test comparing ADCI and SVCI.

[†] APOE genotyping was performed in 246 of 251 participants.

[‡] Patients were considered PiB-positive if their global PiB retention ratio was greater than 1.5.

Values are expressed as mean (standard deviation) or number (%).

2. PiB-PET acquisition

[^{11}C] PiB-PET scanning was performed at Samsung Medical Center or Asan Medical Center using a Discovery STe PET/CT scanner (GE Medical Systems, Milwaukee, WI) in three-dimensional scanning mode with 35 slices at 4.25-mm thickness spanning the entire brain. [^{11}C] PiB was injected into the antecubital vein as a bolus at a mean dose of 420 MBq (i.e., range 259–550 MBq). A CT scan was performed for attenuation correction at 60 minutes after injection. A 30-minute emission static PET scan was initiated. The specific radioactivity of [^{11}C]-PiB at the time of administration was greater than 1500 Ci/mmol for patients, and the radiochemical yield was greater than 35%. The radiochemical purity of the tracer was greater than 95% in all PET studies.

3. PiB-PET data analysis

PiB PET images were co-registered to individual MRIs, normalized to a T1-weighted MRI template. The quantitative regional values of PiB retention on the spatially normalized PiB images were obtained using an automated volume of interest (VOI) analysis drawn from the automated anatomical labeling (AAL) atlas. Data processing was performed using SPM version 5 (SPM5) under Matlab 6.5 (Mathworks, Natick, MA).

To measure PiB retention, we used the cerebral cortical region to cerebellum uptake ratio (UR). The global PiB retention ratio was calculated from the volume-weighted average UR of 28 bilateral cerebral cortical VOIs. Detailed methods for the calculation of global PiB retention ratio are described in online data supplement 2. We defined the PiB retention ratio as a continuous variable indexing amyloid burden.

4. MRI acquisition

MRI was performed with a 3.0 Tesla MRI scanner (Achieva; Philips Medical Systems, Best, The Netherlands) at Samsung Medical Center. Three-dimensional (3D) T1 turbo field echo and 3D fluid-attenuated inversion recovery (FLAIR) were performed for all 251 subjects. Detailed imaging parameters are described in online data supplement 3.

5. Measurement of WMH volume

We quantified WMH volume on FLAIR images using an automated method, as previously described[23]. Due to WMH segmentation errors, WMH volumes could not be calculated for six patients.

6. Lacunae on MRI

Lacunae were defined as small lesions (≥ 3mm and ≤ 15mm in diameter) with low signal on T1-weighted images, high signal on T2-weighted images, and perilesional halo on FLAIR images. Two experienced neurologists blinded to the clinical information reviewed the number and location of lacunae on FLAIR images. The rate of agreement between the two neurologists was 83.0%. Consensus was reached in all cases of discrepancy.

7. Cortical thickness data analysis

T1-weighted images were processed using the standard Montreal Neurological Institute (MNI) anatomic pipeline. Further image processing for cortical thickness is described in online data supplement 4. The individual cortical surface of each subject was registered to the precategorized template and divided into frontal, temporal, parietal, and occipital lobes via automated processes. The averaged values of the thickness of the whole vertices in each hemisphere and lobar region were used for the global analysis. In this way, we obtained mean thickness of the frontal lobe (mean frontal thickness). Intracranial volume (ICV) was defined as the sum of gray matter, white matter, and CSF volume. We included ICV as a covariate to control for the effect of brain size. Nine of 251 patients, (one aMCI, two svMCI, and six SVaD) were excluded from cortical thickness analysis due to registration errors during preprocessing. As a result, data from 242 patients were successfully measured.

8. Hippocampal shape and volume measurement

Hippocampal shape and volume were measured with a surface-based method, described in online data supplement 5. Vertex-wise hippocampal deformation data and hippocampal volume were measured successfully in 238 patients. Due to extraction

error, data for 13 patients (two aMCI, two AD, five svMCI, and four SVaD) could not be obtained.

9. Neuropsychological tests

All patients underwent a standardized neuropsychological battery called the Seoul Neuropsychological Screening Battery (SNSB)[24]. The battery contains tests evaluating attention, language, praxis, four elements of Gerstmann syndrome, visuospatial processing, verbal and visual memory, and executive function. Based on these results, we calculated memory and executive sub-domain scores as described in a previous study[25] and online data supplement 6. The memory scores ranged from 0-150. The executive scores ranged from 0-55.

10. Statistical analysis

To investigate independent effects of global PiB retention ratio, WMH volume, and number of lacunae on mean cortical thickness and hippocampal volume, we entered them as predictors in general linear models controlling for age, gender, education, ICV, and clinical group (ADCI vs. SVCI).

To investigate the topography of cortical thinning and hippocampal deformity associated with global PiB retention ratio, WMH volume, and number of lacunae, we entered the three markers simultaneously in a general linear model as predictors for regional cortical thickness and hippocampal deformity on a vertex-by-vertex basis. Covariates included age, gender, education, ICV, and clinical group. The resulting statistical maps were thresholded after pooling the *p*-values from the regression analyses using the false discovery rate (FDR) theory at a Q value of 0.05. Among the 245 patients with successful WMH volume measurement, eight patients with cortical thickness registration errors and 11 patients with hippocampal extraction errors were further excluded from cortical thickness and hippocampal shape analyses. As a result, data from 237 patients were used for cortical thickness analysis, and data from 234 patients were used for hippocampal shape analysis.

To evaluate the relative effects of amyloid burden and CVD markers on cognition with or without the mediation of brain atrophy, path analysis was performed after controlling for age, gender, education, ICV, and clinical group. Path analysis was

used to simultaneously consider the direct, indirect, and total effects of predictors on outcomes through mediators. Path analyses using memory score and executive score as the outcome variables were performed using hippocampal volume and mean frontal thickness as mediators because the hippocampus is known to be associated with memory function, while the frontal cortex is associated with executive function. PiB retention ratio and WMH are also predominantly associated with hippocampal shape deformities and frontal cortical thinning, respectively. We also entered mean frontal thickness as a mediator for memory scores because frontal impairment is associated with memory dysfunction[26]. Path analysis for memory score was performed using data from 216 patients after excluding 35 patients (six with WMH segmentation errors, eight with registration errors for cortical thickness, 11 with hippocampal extraction errors, and 10 with missing memory score data). Path analysis for executive score was performed using data from 214 patients after excluding 37 patients (six with WMH segmentation errors, eight with registration errors for cortical thickness, and 23 with missing executive score data). These models showed good fit to the memory score ($\chi 2$ = 13.68, df = 16, p = 0.855, CFI > 0.999, RMSEA < 0.001) and executive score ($\chi 2$ = 14.96, df = 16, p = 0.52, CFI > 0.999, RMSEA < 0.001) data.

Amos Version 18.0 software (SPSS, Chicago, Illinois) was used for all path analyses using maximum likelihood estimation.

III. RESULTS

1. Effects of PiB retention ratio, WMH volume, and number of lacunae on cortical thickness

Global PiB retention ratio was not associated with mean cortical thickness (β = -0.05, SE = 0.03, p = 0.067). Higher WMH volume was associated with lower mean cortical thickness (β = -0.002, SE = 0.001, p = 0.033), while the number of lacunae was not (β = -0.001, SE = 0.001, p = 0.331).

Global PiB retention ratio was associated with cortical thinning in bilateral medial and lateral temporal, lateral parietal, and precuneus regions (Figure 1). Higher

WMH volume was associated with cortical thinning in bilateral medial and lateral frontal, lateral temporal, insula, cingulate, and lingual regions. The number of lacunae was not associated with regional cortical thinning.

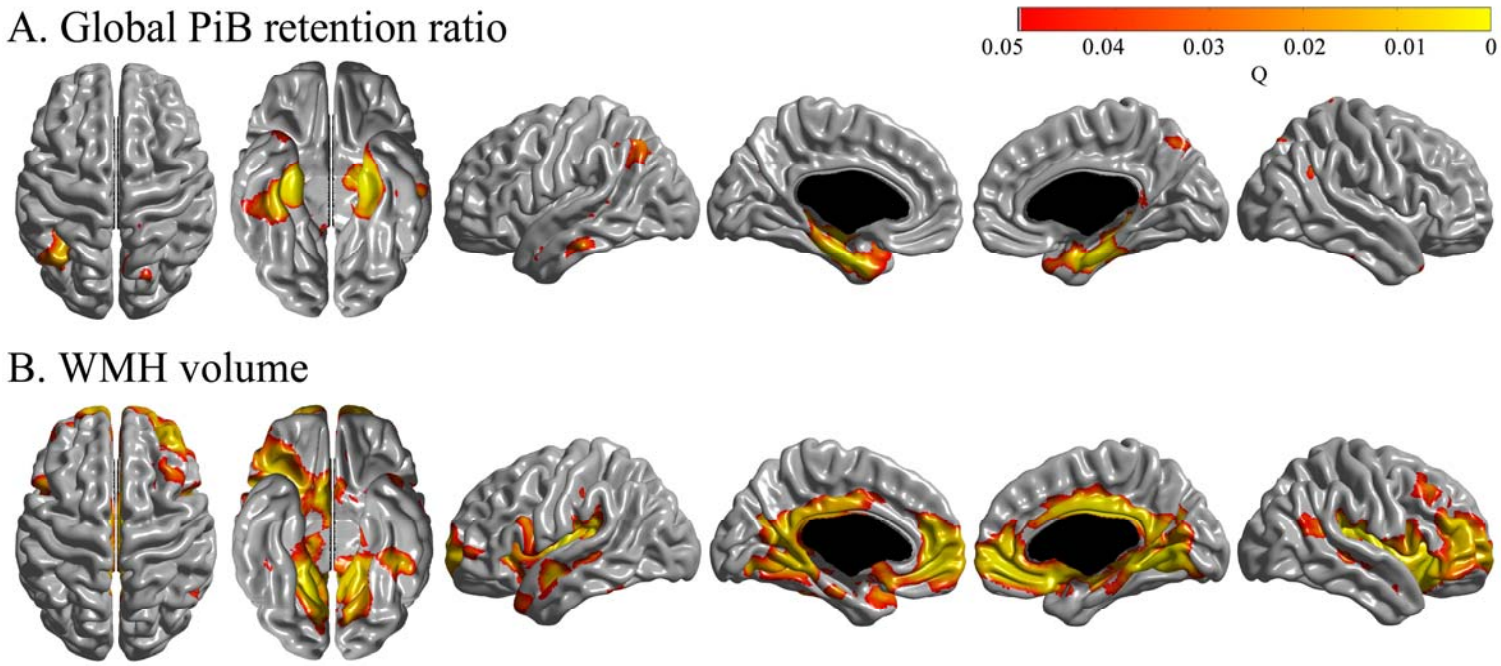

Figure 1. Region of cortical thinning associated with Pittsburgh Compound B (PiB) (A) and white matter hyperintensities (WMH) volume (B). Global PiB retention ratio, WMH volume, and number of lacunae were entered in a general linear model. Age, gender, education, clinical group, and intracranial volume were entered as covariates. Global PiB retention ratio was associated with cortical thinning in bilateral medial, lateral temporal, lateral parietal, and precuneus regions. Higher WMH volume was associated with cortical thinning in bilateral medial and lateral frontal, lateral temporal, insula, cingulate, and lingual regions. The number of lacunae was not associated with regional cortical thinning.

2. Effects of PiB retention ratio, WMH volume, and number of lacunae on hippocampal shape

Global PiB retention ratio was associated with hippocampal volume (β = -0.21, *SE* = 0.06, $p < 0.001$). WMH volume (β = -0.004, *SE* = 0.002, $p = 0.085$) and the number of lacunae (β = 0.001, *SE* = 0.003, $p = 0.838$) were not associated with hippocampal volume.

PiB retention ratio was associated with shape deformities in the superior-lateral heads, bilaterally in the medial and lateral bodies of the hippocampus, in the inferior body of the right hippocampus, and the inferior-medial head of the left side of the hippocampus. WMH volume was associated with shape deformities in the bilateral inferior bodies of the hippocampus and the lateral head and body of the right side of the hippocampus. The number of lacunae was associated with deformity in the lateral body and tail of the right side of the hippocampus (Figure 2).

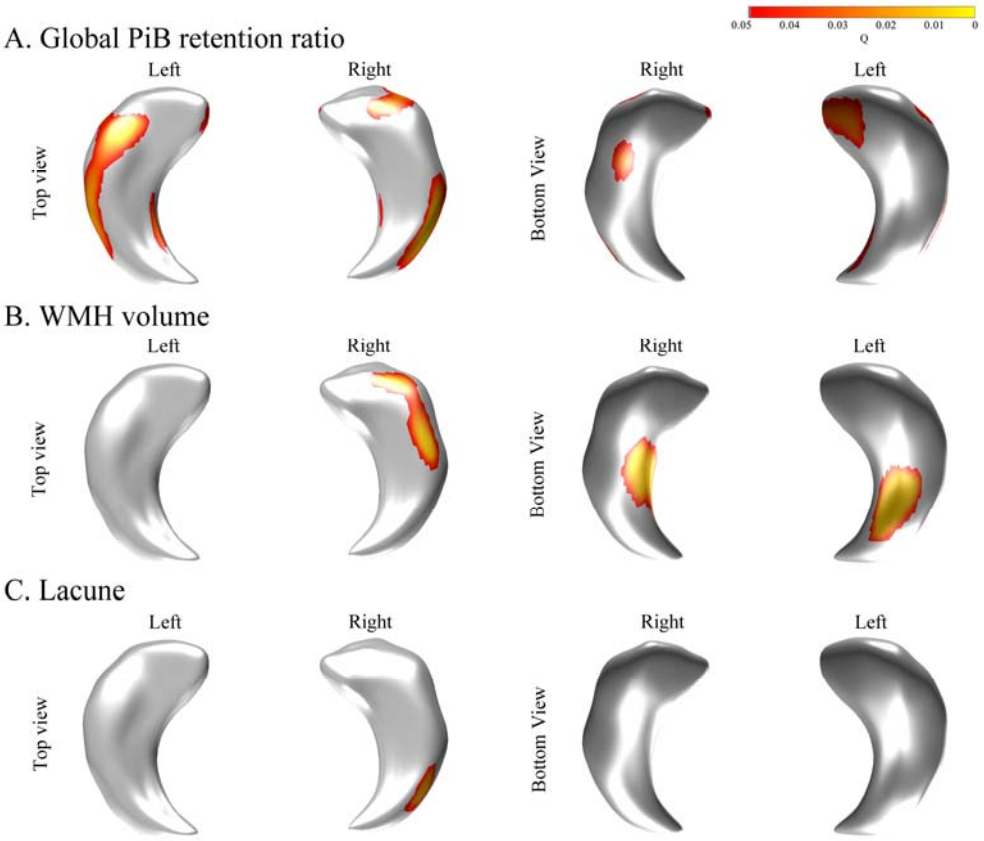

Figure 2. Region of hippocampal deformity associated with global Pittsburgh Compound B (PiB) retention ratio (A), white matter hyperintensities (WMH) volume (B), and number of lacunae (C). Global PiB retention ratio was related to deformity in the superior-lateral heads, bilaterally in the medial and lateral bodies of the hippocampus, in the inferior body of the right side of the hippocampus, and the inferior-medial head of the left side of the hippocampus. WMH volume was associated with deformity in the bilateral inferior bodies of the hippocampus and lateral head and body of the right side of the hippocampus. The number of lacunae was associated with deformity in the lateral body and tail of the right side of the hippocampus. Global PiB retention ratio, WMH volume, and the number of lacunae were entered in a general linear model. Age, gender, education, clinical group, and intracranial volume were entered as covariates.

3. Relationships among PiB retention ratio, CVD markers, brain atrophy, and memory scores

In the path analysis for memory score (Table 2), global PiB retention ratio was associated with mean hippocampal volume (p=0.010), which was further associated with memory function score (p=0.010). Global PiB retention ratio was associated with memory score without mediation of hippocampus volume or mean frontal thickness (p=0.010). WMH were associated with mean frontal thickness (p=0.010), which was further associated with memory function score (p=0.010). Lacunae were associated with memory score without mediation of hippocampus volume or mean frontal thickness (p=0.029) (Figure 3).

Table 3 shows the total effects of PiB retention ratio, lacunae and WMH on memory score; PiB retention ratio and lacunae account for 0.42 and 0.22 of the memory score, respectively. Total effect of WMH on memory score was 0.17, but it was not statistically significant (p=0.091).

Because amyloid burden was associated with brain atrophy in the temporal-parietal region in the cortical thickness analysis, we performed further path analysis on memory score using mean temporal-parietal thickness as a mediator variable (Supplementary Table 1 and Supplementary Figure 1). PiB retention ratio was associated with memory score with and without mediation of mean temporal-parietal thickness.

4. Relationships among PiB retention ratio, CVD markers, brain atrophy, and executive scores

In the path analysis for executive score (Table 2), global PiB retention ratio was associated with executive score without the mediation of mean frontal thickness (p=0.010). WMH were associated with mean frontal thickness (p=0.022), which was further associated with executive score (p=0.010). The number of lacunae was associated with executive score without the mediation of mean frontal thickness (p=0.010) (Figure 3).

Table 3 shows the total effects of PiB retention ratio, lacunae and WMH on executive score; PiB retention ratio, lacunae and WMH account for 0.20, 0.26 and 0.21 of the executive score, respectively.

Table 2. Effects of predictors (PiB retention ratio, WMH volumes and number of lacunae) on cognition (memory and executive scores) through mediators (hippocampal volume and/or mean frontal thickness)

	Path analysis 1									Path analysis 2					
	Hippocampal volume			Mean frontal thickness			Memory score			Mean frontal thickness			Executive score		
	β	*SE*	*p* value	β	*SE*	*p* value	β	*SE*	*p* value	β	*SE*	*p* value	β	*SE*	*p* value
Global PiB retention ratio	-0.20	0.05	0.010	0.002	0.02	0.964	-13.77	2.43	0.010	0.002	0.03	0.908	-4.44	1.41	0.010
WMH volume	-0.004	0.003	0.105	-0.003	0.001	0.010	-0.05	0.09	0.588	-0.003	0.001	0.022	-0.06	0.05	0.309
Lacunae	0.0003	0.002	0.894	-0.001	0.001	0.327	-0.36	0.14	0.029	-0.001	0.002	0.454	-0.22	0.07	0.010
Hippocampal volume							13.60	3.44	0.010						
Mean frontal thickness							24.06	7.31	0.010				21.72	3.27	0.010

Values shown are the results of path analyses for memory score (path analysis 1) and executive score (path analysis 2).
Abbreviations: β, unstandardized beta coefficient; PiB, Pittsburgh compound B; *SE*, standard error; WMH, white matter hyperintensities.

Table 3. Total effects of imaging markers on cognition

Domain	Predictors	Total effect		
		Standardized beta	*SE*	*p* value
Memory score	Global PiB retention ratio	-0.42	0.06	0.010
	WMH volume	-0.17	0.10	0.091
	Lacunae	-0.22	0.08	0.026
Executive score	Global PiB retention ratio	-0.20	0.07	0.010
	WMH volume	-0.21	0.10	0.039
	Lacunae	-0.26	0.07	0.010

Values shown are the results of path analyses for memory score (path analysis 1) and executive score (path analysis 2).
Abbreviations: PiB, Pittsburgh compound B; *SE*, standard error; WMH, white matter hyperintensities.

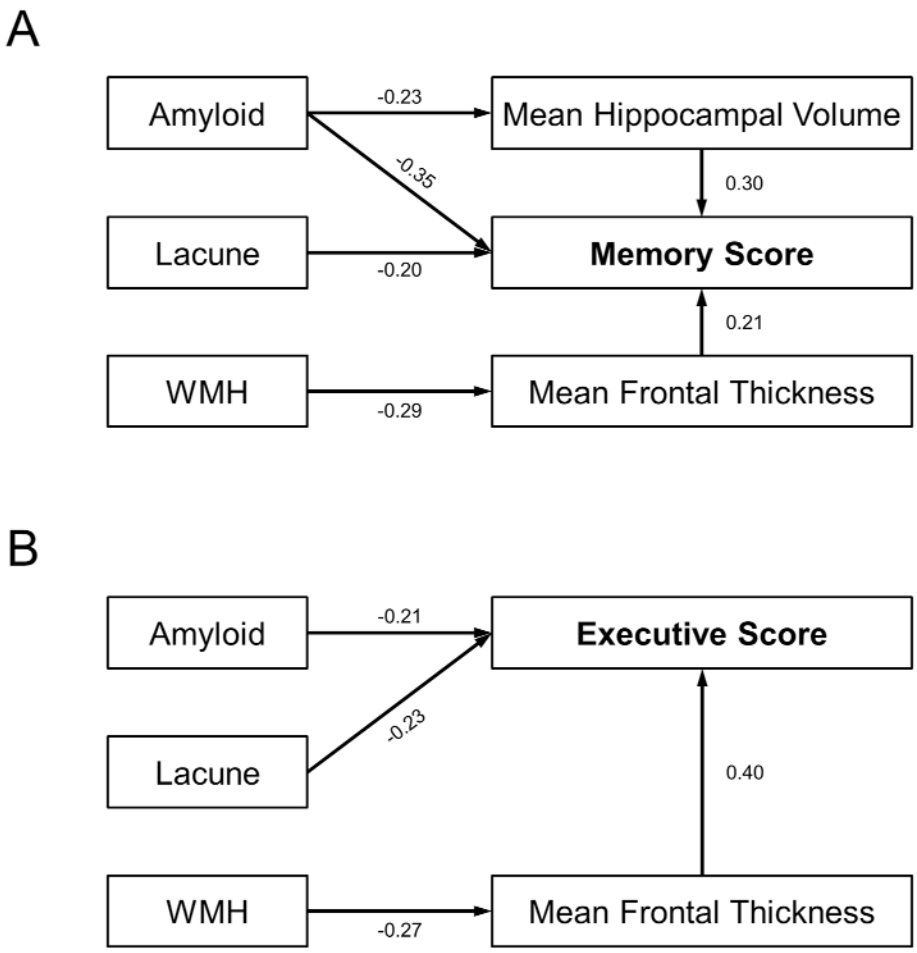

Figure 3. Schematic diagram of the path analyses. Path analysis for memory function score (A) and executive function score (B). Mean hippocampal volume and mean frontal thickness were entered as mediator variables for memory function score. Mean frontal thickness was entered as a mediator variable for executive function score. Amyloid burden, white matter hyperintensities (WMH), and the number of lacunae were entered as predictors. Age, gender, education, clinical group, and intracranial volume were entered as covariates. The numbers on the paths are standardized coefficients. Direct paths that were statistically significant were reported.

IV. DISCUSSION

This study reports new data for potential mechanisms underlying the relationships among amyloid burden, CVD, brain atrophy, and cognitive impairment in a large cohort of carefully phenotyped, cognitively impaired patients using non-invasive amyloid imaging and structural MRI for markers of CVD, cortical thickness, and hippocampal atrophy. The major findings of this study are as follows. First, amyloid burden was found to be associated with the hippocampal atrophy or temporal-parietal thinning, which was further associated with memory impairment. Second, WMH were associated with frontal thinning, which was further associated with executive and memory dysfunctions. Finally, amyloid burden and lacunae were also associated with memory and executive dysfunction without the mediation of hippocampal or frontal atrophy. Taken together, these findings suggest that brain atrophy is the common pathway between amyloid burden or CVD and cognitive impairments. Further, these findings indicate that amyloid burden and CVD affect cognitive impairment without the mediation of brain atrophy.

We found that amyloid burden and CVD independently affect region-specific brain atrophy. That is, PiB retention ratio was associated with cortical thinning in the medial and lateral temporal, lateral parietal, and precuneus regions. Further, the PiB retention ratio was associated with hippocampal atrophy, especially in the superior-lateral and inferior-medial portions of the head and body, which corresponded to the cornu ammonis (CA) 1 and subiculum[27]. The topography of hippocampal shape deformities and cortical thinning are consistent with previous studies of AD patients[28-30].

WMH were associated with cortical thinning in the frontal, perisylvian, and lingual regions. Previous studies showed that WMH were associated with brain atrophy[13,15], and a more recent study evaluated the topography of cortical thinning related to WMH volume[12]. However, unlike previous studies, our findings suggest that WMH are responsible for cortical thinning in these regions regardless of the effects of amyloid burden and lacunae. In this study, there was no association between lacunae and cortical atrophy. Previous studies have shown inconsistent results on the relationship between the number of lacunae and cortical atrophy[31,32]. One study on

patients with CADASIL showed that lacuna burden was associated with cortical changes[31]. However, these findings are inconsistent with a previous study of cognitively impaired patients with varying degrees of CVD, which is similar to the subjects in this study, suggesting that WMH had a significant effect on cortical gray matter volume, but lacunae did not[13]. We also found that WMH and lacunae were associated with shape deformities in the superior lateral head and body (CA1) and inferior body (CA 1 and subiculum) and superior lateral body (CA1) of the hippocampus, respectively. These subregions are known to be susceptible to ischemia[33].

Our first conclusion that brain atrophy is the common pathway between amyloid or CVD and cognitive impairments is supported by the following observations: (1) amyloid burden was associated with the temporal-parietal thinning including hippocampal atrophy, which was further associated with memory impairment; (2) WMH was associated with frontal thinning, which was further associated with executive and memory dysfunctions. Although several studies have shown that amyloid burden and CVD were independently associated with cognitive impairment[11,18], most studies did not evaluate the mediative effects of brain atrophy on the relationships between amyloid burden or CVD and cognitive impairments. A recent study showed that amyloid burden affected hippocampal atrophy, which in turn led to memory dysfunction[11]. One previous study from our group revealed that WMH were associated with frontal thinning, which is further associated with executive dysfunction[12]. Therefore, our findings suggest that amyloid burden and CVD might affect memory and executive dysfunction through hippocampal and frontal atrophy, respectively.

We found that WMH affected memory dysfunction with mediation of frontal thinning. WMH are known to involve frontal-subcortical circuits responsible for not only executive, but also memory dysfunction[34]. Indeed, previous studies have revealed that WMH[35] as well as frontal lesions[36] were associated with memory dysfunction.

Our study provides new evidence that amyloid burden is also associated with memory and executive dysfunction without mediation of hippocampal or frontal atrophy. There have been only a few studies evaluating the relationships among

amyloid burden, the hippocampus, and memory function[11]. Unlike the present findings, these previous studies suggested that amyloid burden affected memory dysfunction through the mediation of hippocampal atrophy. This discrepancy might be due to differences in study population (MCI or dementia patients with varying degrees of ischemia in our sample compared to non-demented subjects with mild degrees of ischemia in the previous study).

Amyloid burden had significant effect on cognition without the mediation of hippocampal atrophy or frontal thinning (Figure 3). Also, amyloid burden had significant effect on memory function without the mediation of temporal-parietal thinning. The direct effects of amyloid burden on cognition without the mediation of brain atrophy may be due to the fact that amyloid burden affects cortical synaptic/network dysfunction. Indeed, previous studies have shown that amyloid burden affects the default mode network[37,38], which is associated with memory dysfunction[37]. Additionally, amyloid burden may affect functional networks involving the frontal lobes because amyloid burden is distributed predominantly in the frontal regions[37]. Our suggestion seems to be supported by previous studies that have found that the PiB retention ratio is associated with executive dysfunction as well as memory dysfunction in non-demented subjects[39]. Also, previous studies have shown that synaptic/network dysfunction precedes cortical thinning[40]. Therefore, it is possible that amyloid burden might affect synaptic/network dysfunction without brain atrophy. Future studies are needed to investigate this hypothesis. Alternatively, amyloid burden might have affected memory or executive function through atrophy in brain regions that were not considered in the current path analyses.

We also found that lacunae, like WMH, affected executive and memory dysfunctions. However, in contrast to WMH, the effects of lacunae on cognition occurred without the mediation of frontal thinning. Further, the relative effects of lacunae on cognition were greater than those of WMH. For example, the relative effect of lacunae on executive dysfunctions was 0.26, while that of WMH was 0.21. The reason that the effects of WMH on cortical thinning were greater than those of lacunae, while the effects of lacunae on cognition were greater than those of WMH remains unknown. However, this might be related to differences in the topography and severity of involvement between WMH and lacuna. Specifically, WMH usually

involves widespread white matter regions that contain long association fasciculi that connect various cortical regions. However, most lacunae occur focally in subcortical gray matter[13] that does not traverse via a long association fasciculus but that are major structures in frontal-subcortical circuits, associated with cognitive impairments[34]. Also, lacunae reflect a complete infarction, while WMH reflect incomplete ischemic injury[3]. Therefore, WMH affect long association fasciculi, which in turn lead to the secondary degeneration of cortical thinning, while lacunae cause a complete obstruction in major structures in frontal subcortical circuits, which leads to cognitive impairment.

When the relative amount of amyloid influence and CVD markers on cognition were compared after controlling for each other, amyloid burden (0.42) had a greater impact on memory dysfunction than CVD (lacunae, 0.22). In contrast, the total effect of CVD (0.47) on executive dysfunction (lacunae (0.26) and WMH (0.21)) was greater than that of amyloid burden (0.20). Although these findings are consistent with general concepts, interestingly, the effects of amyloid burden on executive dysfunction and the effects of CVD on memory dysfunction were greater than expected. This finding might be explained by the fact that AD and SVaD patients were included as subjects. In AD patients, executive dysfunction is the domain generally affected subsequent to the memory domain[9]. SVaD patients also commonly show memory dysfunction[3]. These findings, however, support previous studies showing that AD and CVD pathologies independently affected cognitive decline and the risk of dementia[6,8,41,42].

This study had several limitations. First, the patients in this study all had cognitive impairment, which may limit the generalizability of these results to other populations. Second, it would be more relevant for predicting the clinical impact of CVD to use the location and volume of lacunae and voxel symptom lesion mapping of WMH rather than just volume or number alone[43]. Third, other pathologies such as tau, cortical microinfarct, or hippocampal sclerosis were not taken into consideration because a pathological study was not performed. Fourth, there is a possibility that the effects of WMH volume and lacunae were not completely disentangled. Although the effects of WMH volume and lacunae were adjusted for each other, the independent effects of WMH volume and lacunae should be cautiously interpreted. Fifth, neuropsychological composite scores used in this study might not purely reflect

memory or executive functions because assessment of neuropsychological performance usually requires integration of multiple cognitive domains[44,45]. Finally, we cannot exclude the possibility that confounding factors could have been introduced by the criteria used to define the clinical groups. These patients, however, were diagnosed using clinical criteria not PiB status. Also, after including clinical criteria as covariates, these findings were unchanged. Therefore, we believe these findings were unlikely to be affected by the criteria used to define each clinical group.

V. CONCLUSION

Our results indicate that amyloid burden and CVD have independent effects on cognitive dysfunction with or without the mediation of specific regional brain atrophy.

REFERENCES

1. Ott A, Breteler MM, van Harskamp F, Claus JJ, van der Cammen TJ, Grobbee DE, et al. Prevalence of Alzheimer's disease and vascular dementia: association with education. The Rotterdam study. BMJ 1995;310:970-3.
2. Gorelick PB. Risk factors for vascular dementia and Alzheimer disease. Stroke 2004;35:2620-2.
3. Roman GC, Erkinjuntti T, Wallin A, Pantoni L, Chui HC. Subcortical ischaemic vascular dementia. Lancet Neurol 2002;1:426-36.
4. Lim A, Tsuang D, Kukull W, Nochlin D, Leverenz J, McCormick W, et al. Clinico-neuropathological correlation of Alzheimer's disease in a community-based case series. J Am Geriatr Soc 1999;47:564-9.
5. Pathological correlates of late-onset dementia in a multicentre, community-based population in England and Wales. Neuropathology Group of the Medical Research Council Cognitive Function and Ageing Study (MRC CFAS). Lancet 2001;357:169-75.
6. Schneider JA, Wilson RS, Bienias JL, Evans DA, Bennett DA. Cerebral infarctions and the likelihood of dementia from Alzheimer disease pathology. Neurology 2004;62:1148-55.
7. Bennett DA, Schneider JA, Arvanitakis Z, Kelly JF, Aggarwal NT, Shah RC, et al. Neuropathology of older persons without cognitive impairment from two community-based studies. Neurology 2006;66:1837-44.
8. Chui HC, Zarow C, Mack WJ, Ellis WG, Zheng L, Jagust WJ, et al. Cognitive impact of subcortical vascular and Alzheimer's disease pathology. Ann Neurol 2006;60:677-87.
9. Reed BR, Mungas DM, Kramer JH, Ellis W, Vinters HV, Zarow C, et al. Profiles of neuropsychological impairment in autopsy-defined Alzheimer's disease and cerebrovascular disease. Brain 2007;130:731-9.
10. Marchant NL, Reed BR, Sanossian N, Madison CM, Kriger S, Dhada R, et al. The aging brain and cognition: contribution of vascular injury and abeta to mild cognitive dysfunction. JAMA Neurol 2013;70:488-95.
11. Mormino EC, Kluth JT, Madison CM, Rabinovici GD, Baker SL, Miller BL, et al. Episodic memory loss is related to hippocampal-mediated beta-amyloid

deposition in elderly subjects. Brain 2009;132:1310-23.
12. Seo SW, Lee JM, Im K, Park JS, Kim SH, Kim ST, et al. Cortical thinning related to periventricular and deep white matter hyperintensities. Neurobiol Aging 2012;33:1156-67.
13. Du AT, Schuff N, Chao LL, Kornak J, Ezekiel F, Jagust WJ, et al. White matter lesions are associated with cortical atrophy more than entorhinal and hippocampal atrophy. Neurobiol Aging 2005;26:553-9.
14. Becker JA, Hedden T, Carmasin J, Maye J, Rentz DM, Putcha D, et al. Amyloid-beta associated cortical thinning in clinically normal elderly. Ann Neurol 2011;69:1032-42.
15. Schmidt R, Ropele S, Enzinger C, Petrovic K, Smith S, Schmidt H, et al. White matter lesion progression, brain atrophy, and cognitive decline: the Austrian stroke prevention study. Ann Neurol 2005;58:610-6.
16. Mungas D, Jagust WJ, Reed BR, Kramer JH, Weiner MW, Schuff N, et al. MRI predictors of cognition in subcortical ischemic vascular disease and Alzheimer's disease. Neurology 2001;57:2229-35.
17. Jokinen H, Lipsanen J, Schmidt R, Fazekas F, Gouw AA, van der Flier WM, et al. Brain atrophy accelerates cognitive decline in cerebral small vessel disease: the LADIS study. Neurology 2012;78:1785-92.
18. Whitwell JL, Josephs KA, Murray ME, Kantarci K, Przybelski SA, Weigand SD, et al. MRI correlates of neurofibrillary tangle pathology at autopsy: a voxel-based morphometry study. Neurology 2008;71:743-9.
19. McKhann G, Drachman D, Folstein M, Katzman R, Price D, Stadlan EM. Clinical diagnosis of Alzheimer's disease: report of the NINCDS-ADRDA Work Group under the auspices of Department of Health and Human Services Task Force on Alzheimer's Disease. Neurology 1984;34:939-44.
20. Erkinjuntti T, Inzitari D, Pantoni L, Wallin A, Scheltens P, Rockwood K, et al. Research criteria for subcortical vascular dementia in clinical trials. J Neural Transm Suppl 2000;59:23-30.
21. Seo SW, Cho SS, Park A, Chin J, Na DL. Subcortical vascular versus amnestic mild cognitive impairment: comparison of cerebral glucose metabolism. J Neuroimaging 2009;19:213-9.

22. Fazekas F, Chawluk JB, Alavi A, Hurtig HI, Zimmerman RA. MR signal abnormalities at 1.5 T in Alzheimer's dementia and normal aging. AJR Am J Roentgenol 1987;149:351-6.
23. Jeon S, Yoon U, Park J-S, Seo SW, Kim J-H, Kim ST, et al. Fully automated pipeline for quantification and localization of white matter hyperintensity in brain magnetic resonance image. International Journal of Imaging Systems and Technology 2011;21:193-200.
24. Kang Y, Na DL. Seoul Neuropsychological Screening Battery (SNSB). Incheon: Human Brain Research & Consulting Co.; 2003.
25. Ahn HJ, Chin J, Park A, Lee BH, Suh MK, Seo SW, et al. Seoul Neuropsychological Screening Battery-dementia version (SNSB-D): a useful tool for assessing and monitoring cognitive impairments in dementia patients. J Korean Med Sci 2010;25:1071-6.
26. Reed BR, Eberling JL, Mungas D, Weiner M, Kramer JH, Jagust WJ. Effects of white matter lesions and lacunes on cortical function. Arch Neurol 2004;61:1545-50.
27. Apostolova LG, Dutton RA, Dinov ID, Hayashi KM, Toga AW, Cummings JL, et al. Conversion of mild cognitive impairment to Alzheimer disease predicted by hippocampal atrophy maps. Arch Neurol 2006;63:693-9.
28. Wang L, Miller JP, Gado MH, McKeel DW, Rothermich M, Miller MI, et al. Abnormalities of hippocampal surface structure in very mild dementia of the Alzheimer type. Neuroimage 2006;30:52-60.
29. Gerardin E, Chetelat G, Chupin M, Cuingnet R, Desgranges B, Kim HS, et al. Multidimensional classification of hippocampal shape features discriminates Alzheimer's disease and mild cognitive impairment from normal aging. Neuroimage 2009;47:1476-86.
30. Bakkour A, Morris JC, Dickerson BC. The cortical signature of prodromal AD: regional thinning predicts mild AD dementia. Neurology 2009;72:1048-55.
31. Jouvent E, Mangin JF, Porcher R, Viswanathan A, O'Sullivan M, Guichard JP, et al. Cortical changes in cerebral small vessel diseases: a 3D MRI study of cortical morphology in CADASIL. Brain 2008;131:2201-8.

32. Kloppenborg RP, Nederkoorn PJ, Grool AM, Vincken KL, Mali WP, Vermeulen M, et al. Cerebral small-vessel disease and progression of brain atrophy: the SMART-MR study. Neurology 2012;79:2029-36.
33. Kirino T, Sano K. Selective vulnerability in the gerbil hippocampus following transient ischemia. Acta Neuropathol 1984;62:201-8.
34. Cummings JL. Frontal-subcortical circuits and human behavior. Arch Neurol 1993;50:873-80.
35. Au R, Massaro JM, Wolf PA, Young ME, Beiser A, Seshadri S, et al. Association of white matter hyperintensity volume with decreased cognitive functioning: the Framingham Heart Study. Arch Neurol 2006;63:246-50.
36. Wheeler MA, Stuss DT, Tulving E. Frontal lobe damage produces episodic memory impairment. J Int Neuropsychol Soc 1995;1:525-36.
37. Sperling RA, Laviolette PS, O'Keefe K, O'Brien J, Rentz DM, Pihlajamaki M, et al. Amyloid deposition is associated with impaired default network function in older persons without dementia. Neuron 2009;63:178-88.
38. Sheline YI, Raichle ME, Snyder AZ, Morris JC, Head D, Wang S, et al. Amyloid plaques disrupt resting state default mode network connectivity in cognitively normal elderly. Biol Psychiatry 2010;67:584-7.
39. Resnick SM, Sojkova J, Zhou Y, An Y, Ye W, Holt DP, et al. Longitudinal cognitive decline is associated with fibrillar amyloid-beta measured by [11C]PiB. Neurology 2010;74:807-15.
40. Sperling RA, Aisen PS, Beckett LA, Bennett DA, Craft S, Fagan AM, et al. Toward defining the preclinical stages of Alzheimer's disease: recommendations from the National Institute on Aging-Alzheimer's Association workgroups on diagnostic guidelines for Alzheimer's disease. Alzheimers Dement 2011;7:280-92.
41. Schneider JA, Arvanitakis Z, Bang W, Bennett DA. Mixed brain pathologies account for most dementia cases in community-dwelling older persons. Neurology 2007;69:2197-204.
42. Schneider JA, Boyle PA, Arvanitakis Z, Bienias JL, Bennett DA. Subcortical infarcts, Alzheimer's disease pathology, and memory function in older persons. Ann Neurol 2007;62:59-66.

43. Duering M, Zieren N, Herve D, Jouvent E, Reyes S, Peters N, et al. Strategic role of frontal white matter tracts in vascular cognitive impairment: a voxel-based lesion-symptom mapping study in CADASIL. Brain 2011;134:2366-75.
44. Sweet JJ, Suchy Y, Leahy B, Abramowitz C, Nowinski CJ. Normative clinical relationships between orientation and memory: age as an important moderator variable. Clin Neuropsychol 1999;13:495-508.
45. Kipps CM, Hodges JR. Cognitive assessment for clinicians. J Neurol Neurosurg Psychiatry 2005;76 Suppl 1:i22-30.

APPENDICES

Supplementary Text 1

Center-specific definitions of amnestic mild cognitive impairment (aMCI) and subcortical vascular MCI (svMCI)

aMCI patients all met Petersen criteria for MCI with these modifications [1]: (1) subjective memory complaint by the patient or his/her caregiver; (2) normal general cognitive function above the 16th percentile on the Korean MMSE; (3) normal activities of daily living as judged by both an interview with a clinician and the standardized ADL scale previously described; (4) objective memory decline below the 16th percentile on neuropsychological tests; and (5) not demented. In addition, we assured that patients had minimal white matter hyperintensity (WMH) on MRI: periventricular WMH < 5mm and deep WMH < 10mm in maximum diameter.

svMCI patients met the following modified Petersen's criteria[1]: (1) subjective cognitive complaint by the patient or his/her caregiver; (2) normal general cognitive function above the 16th percentile on the Korean MMSE; (3) normal activities of daily living as judged by both an interview with a clinician and the standardized ADL scale previously described; (4) objective cognitive decline below the 16th percentile on neuropsychological tests; and (5) not demented. Additionally, all svMCI patients had focal neurological symptoms or signs and significant ischemic changes on MRI. Focal neurological symptoms and signs included corticobulbar signs (facial palsy, dysarthria, dysphagia, or pathologic laughing or crying), pyramidal signs (hemiparesis, hyperactive deep tendon reflexes, or extensor plantar responses), or Parkinsonism (short-step gait, festination, shuffling gait, decreased arm swing while walking, rigidity, bradykinesia, or postural instability). The presence of significant ischemic changes associated with small-vessel disease was defined as WMH on MRI: periventricular WMH (caps and rim) longer than 10mm and deep WMH $\geq$ 25mm in maximum diameter. When defining deep WMH, WMH located within the four axial slices just above the top of the lateral ventricles were considered to be periventricular WMH, while WMH in the fifth or higher axial slices above the top of the lateral ventricle were considered to be deep WMH. These imaging criteria indicate that our svMCI patients had ischemia sufficiently significant to meet at least grade 3 of Fazekas ischemia criteria[2].

Supplementary Text 2

Calculation of global PiB retention ratio

PiB PET images were co-registered to individual MRIs, which were normalized to a T1-weighted MRI template. Using these parameters, MRI co-registered PiB PET images were normalized to the MRI template. The quantitative regional values of PiB retention on the spatially normalized PiB images were obtained by automated VOIs analysis using an automated anatomical labeling (AAL) atlas. Data processing was performed using SPM Version 5 (SPM5) within Matlab 6.5 (MathWorks, Natick, MA).

To measure PiB retention, the cerebral cortical region to cerebellum uptake ratio (UR) was used. The cerebellum was used as a reference region as it did not show group differences. We selected 28 cortical VOIs from left and right hemispheres using the AAL atlas. The cerebral cortical VOIs chosen for this study were the bilateral frontal (superior and middle frontal gyri; medial portion of the superior frontal gyrus; opercular portion of the inferior frontal gyrus; triangular portion of the inferior frontal gyrus; supplementary motor area; orbital portion of the superior, middle, and inferior orbital frontal gyri; rectus and olfactory cortex), posterior cingulate gyri, parietal (superior and inferior, supramarginal and angular gyri, and precuneus), lateral temporal (superior, middle, and inferior temporal gyri, and heschl gyri), and occipital (superior, middle, and inferior occipital gyri, cuneus, calcarine fissure, and lingual, and fusiform gyri). Regional cerebral cortical URs were calculated by dividing each cortical VOI's UR by the mean uptake of the cerebellar cortex (cerebellum crus1 and crus2). Global PiB uptake ratio was calculated from the volume-weighted average UR of 28 bilateral cerebral cortical VOIs. We defined PiB uptake ratio as a continuous variable. Patients were considered PiB-positive if their global PiB uptake ratio was more than two standard deviations (PiB retention ratio > 1.5) from the mean of the normal controls.

Supplementary Text 3

Imaging parameters for MRI acquisition

We acquired 3D T1 turbo field echo MR images with the following imaging parameters: sagittal slice thickness, 1.0 mm, over contiguous slices with 50% overlap; no gap; repetition time (TR) of 9.9 msec; echo time (TE) of 4.6 msec; flip angle of 8°; and matrix size of 240 × 240 pixels, reconstructed to 480 × 480 over a field of view (FOV) of 240 mm. The following parameters were used for the 3D FLAIR images: axial slice thickness of 2 mm; no gap; TR of 11000 msec; TE of 125 msec; flip angle of 90°; and matrix size of 512 × 512 pixels.

Supplementary Text 4

Image processing for cortical thickness measurement

Native MRI images were linearly transformed and registered into a standardized stereotaxic space[3]. The N3 algorithm was used to correct images for intensity-based non-uniformities[4] caused by nonhomogeneities in the magnetic field. Then, the registered and corrected images were classified into white matter, gray matter, CSF, and background using a 3D stereotaxic brain mask and the Intensity-Normalized Stereotaxic Environment for Classification of Tissues (INSECT) algorithm[5]. The surfaces of the inner and outer cortices were automatically extracted using the Constrained Laplacian-Based Automated Segmentation with Proximities (CLASP) algorithm[6].

Because of limitations in linear stereotaxic normalization, cortical thickness was calculated in native space rather than Talairach space. As we transformed MR volumes in native space into stereotaxic space with a linear transformation matrix, the inverse transformation matrix was applied to cortical thickness models to reconstruct them in native space[7]. Cortical thickness was defined as the Euclidean distance between linked vertices of inner and outer surfaces[6]. Thickness value was spatially normalized using surface-based two-dimensional registration with a sphere-to-sphere warping algorithm. Thus, vertices of each subject were nonlinearly registered to a standard surface template[8,9]. Cortical thickness was subsequently smoothed using a surface-based diffusion kernel in order to increase signal-to-noise ratio. We chose a kernel size of 20 mm full-width at half-maximum in order to maximize statistical power while minimizing false positives[10]. For global and lobar regional analyses, the data of 30 normal subjects who had previously been manually categorized to lobes with high inter-rater reliability[11] were registered to the template. The template then used the label of maximum probability in each vertex.

The presence of extensive WMH in MRI scans made it difficult to completely delineate the inner cortical surface with the correct topology due to tissue classification errors. To overcome this technical limitation, we automatically defined the WMH region using a FLAIR image and substituted it for the intensity of peripheral, normal-appearing tissue on the high-resolution T1 image after affine co-registration, as described in an earlier study[12].

Supplementary Text 5

Image processing for hippocampal shape and volume measurement

Hippocampal shape analysis was based on boundary surfaces rather than volume measurement. Surface-based shape analysis and volume measurement have several advantages compared to volume-based approaches[13,14]. Thus, the boundary surfaces of the hippocampi were used to measure hippocampal volume, instead of voxel number. T1 images were processed to perform anatomical parcellations of each subject's hippocampus using the FreeSurfer software package (Version 5.0; Athinoula A. Martinos Center at Massachusetts General Hospital, Harvard Medical School; http:// surfer.nmr.mgh.harvard.edu/). Labeled images with parcellation were transformed into the native anatomical space of the input MRI data. Subcortical mesh surfaces were then extracted from the labeled images for each subject using a Laplacian-based surface modeling system[15]. Next, every surface mesh from the population was registered to the mean surface mesh, which was used as a template mesh[16]. This surface registration provided vertex correspondences for hippocampal surface meshes. Thus, relative deformation of the hippocampal surface meshes against the template was calculated for each vertex. Based on this deformation data, subcortical surface volume was measured employing an algorithm proposed in a previous study[17].

Supplementary Text 6

Neuropsychological tests and calculation of composite scores for frontal and memory function

All patients underwent a standardized neuropsychological battery called the Seoul Neuropsychological Screening Battery (SNSB)[18]. This battery contains tests evaluating attention, language, praxis, four elements of Gerstmann syndrome, visuospatial processing, verbal and visual memory, and frontal/executive function. These included digit span forward/backward, Korean version of the Boston Naming Test, Rey-Osterrieth Complex Figure Test (RCFT: copying, immediate and 20-min delayed recall, and recognition), the Seoul Verbal Learning Test (SVLT: three learning-free recall trials of 12 words, 20-min delayed recall trial for these 12 items, and a recognition test), phonemic and semantic Controlled Oral Word Association Test (COWAT), the Stroop Test (word and color reading of 112 items during a 2-min period), the Mini-Mental State Examination (MMSE), and Clinical Dementia Rating Sum of Boxes (CDR-SOB).

Using results from the SNSB, memory and frontal/executive sub-domain scores were calculated as described in a previous study[19]. Memory-domain SNSB-D score (memory subscore) was calculated by summing scores of orientation, verbal memory, and visual memory tests. Memory subscores ranged from 0-150. Frontal/executive-domain SNSB-D score (frontal subscore) was calculated by summing scores from a category word generation task (COWAT for animal), a phonemic word generation task (phonemic COWAT), and Stroop color reading test. The frontal subscores ranged from 0-55.

Supplementary Table 1. Effects of predictors (PiB retention ratio, WMH volume and number of lacunae) on memory score through mean temporal-parietal thickness

	Mean temporal-parietal thickness			Memory score		
	β	*SE*	*p* value	β	*SE*	*p* value
Global PiB retention ratio	-0.070	0.025	0.015	-13.536	2.413	0.010
WMH volume	-0.002	0.001	0.024	-0.078	0.093	0.435
Lacunae	-0.001	0.001	0.341	-0.333	0.139	0.040
Mean temporal-parietal thickness				41.986	6.369	0.010

Values shown are the results of path analyses.
Abbreviations: β, unstandardized beta coefficient; PiB, Pittsburgh compound B; *SE*, standard error; WMH, white matter hyperintensities.

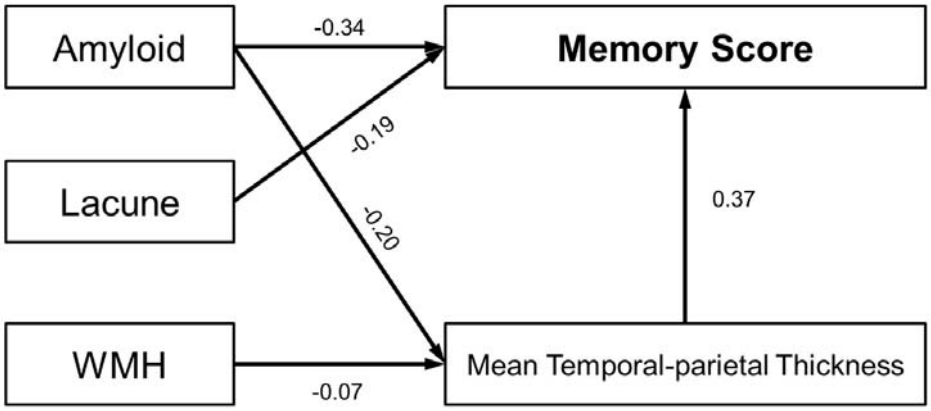

Supplementary Figure 1. Schematic diagram of additional path analysis for memory score.
Results of path analysis for memory function score. Mean temporal-parietal thickness was entered as a mediator variable. Amyloid burden, white matter hyperintensities (WMH), and the number of lacunae were entered as predictors. Age, gender, education, intracranial volume, and clinical group were entered as covariates. Numbers on the paths are standardized beta coefficients. Statistically significant direct paths were expressed.
Abbreviations: SNSBD, Seoul Neuropsychological Screening Battery Domain.

Supplementary References

1. Seo SW, Cho SS, Park A, Chin J, Na DL. Subcortical vascular versus amnestic mild cognitive impairment: comparison of cerebral glucose metabolism. J Neuroimaging 2009;19:213-9.
2. Fazekas F, Chawluk JB, Alavi A, Hurtig HI, Zimmerman RA. MR signal abnormalities at 1.5 T in Alzheimer's dementia and normal aging. AJR Am J Roentgenol 1987;149:351-6.
3. Collins DL, Neelin P, Peters TM, Evans AC. Automatic 3D intersubject registration of MR volumetric data in standardized Talairach space. J Comput Assist Tomogr 1994;18:192-205.
4. Sled JG, Zijdenbos AP, Evans AC. A nonparametric method for automatic correction of intensity nonuniformity in MRI data. IEEE Trans Med Imaging 1998;17:87-97.
5. Zijdenbos A, Evans A, Riahi F, Sled J, Chui J, Kollokian V. Visualization in Biomedical Computing.
6. Kim JS, Singh V, Lee JK, Lerch J, Ad-Dab'bagh Y, MacDonald D, et al. Automated 3-D extraction and evaluation of the inner and outer cortical surfaces using a Laplacian map and partial volume effect classification. Neuroimage 2005;27:210-21.
7. Im K, Lee JM, Lee J, Shin YW, Kim IY, Kwon JS, et al. Gender difference analysis of cortical thickness in healthy young adults with surface-based methods. Neuroimage 2006;31:31-8.
8. Lyttelton O, Boucher M, Robbins S, Evans A. An unbiased iterative group registration template for cortical surface analysis. Neuroimage 2007;34:1535-44.
9. Robbins S, Evans AC, Collins DL, Whitesides S. Tuning and comparing spatial normalization methods. Med Image Anal 2004;8:311-23.
10. Chung MK, Worsley KJ, Robbins S, Paus T, Taylor J, Giedd JN, et al. Deformation-based surface morphometry applied to gray matter deformation. Neuroimage 2003;18:198-213.
11. Romero-Corral A, Montori VM, Somers VK, Korinek J, Thomas RJ, Allison TG, et al. Association of bodyweight with total mortality and with cardiovascular events in coronary artery disease: a systematic review of cohort studies. Lancet 2006;368:666-78.
12. Jeon S, Yoon U, Park J-S, Seo SW, Kim J-H, Kim ST, et al. Fully automated pipeline for quantification and localization of white matter hyperintensity in brain magnetic resonance image. International Journal of Imaging Systems and Technology 2011;21:193-200.
13. Thompson PM, Hayashi KM, De Zubicaray GI, Janke AL, Rose SE, Semple J, et al. Mapping hippocampal and ventricular change in Alzheimer disease. Neuroimage 2004;22:1754-66.
14. Wang L, Miller JP, Gado MH, McKeel DW, Rothermich M, Miller MI, et al. Abnormalities of hippocampal surface structure in very mild dementia of the Alzheimer type. Neuroimage 2006;30:52-60.
15. Kim J, Park J. Organ Shape Modeling Based on the Laplacian Deformation Framework for Surface-Based Morphometry Studies. Journal of Computing Science and Engineering 2012:219-26.

16. Cho Y, Seong JK, Shin SY, Jeong Y, Kim JH, Qiu A, et al. A multi-resolution scheme for distortion-minimizing mapping between human subcortical structures based on geodesic construction on Riemannian manifolds. Neuroimage 2011;57:1376-92.
17. Alyassin AM, Lancaster JL, Downs JH, 3rd, Fox PT. Evaluation of new algorithms for the interactive measurement of surface area and volume. Med Phys 1994;21:741-52.
18. Kang Y, Na DL. Seoul Neuropsychological Screening Battery: Professional Manual. Seoul: Human Brain Research & Consulting Co.; 2003.
19. Ahn HJ, Chin J, Park A, Lee BH, Suh MK, Seo SW, et al. Seoul Neuropsychological Screening Battery-dementia version (SNSB-D): a useful tool for assessing and monitoring cognitive impairments in dementia patients. J Korean Med Sci 2010;25:1071-6.

ABSTRACT(IN KOREAN)

인지기능 저하환자에서의 아밀로이드의 양, 뇌혈관 질환, 뇌위축 및 인지기능

<지도교수 손 영 호 >

연세대학교 대학원 의학과

예 병 석

배경: 알츠하이머 병(Alzheimer's disease)과 피질하 혈관성 치매(Subcortical vascular dementia)는 노인에서의 흔한 퇴행성 치매의 원인으로 흔하게 동반되는 것으로 알려져 있다. 알츠하이머 병리와 뇌혈관질환(cerebrovascular disease) 병리가 독립적으로 뇌의 구조적 변화 및 인지기능 저하에 미치는 영향을 조사하였다.

방법: 총 251명의 인지기능저하 환자(45명의 기억성 경도인지장애, 69명의 알츠하이머 치매, 67명의 피질하 혈관성 경도인지장애, 70명의 피질하 혈관성 치매)를 대상으로 뇌 자기공명영상, 아밀로이드 페트(Pittsburgh Compound B Positron Emission Tomography), 및 신경심리검사를 시행하였다. 자기공명영상을 바탕으로 뇌혈관질환 병리의 뇌영상마커인 white matter hyperintensities(WMH) 및 열공성 뇌경색(lacunar infarction)의 양 및 뇌위축의 정도(뇌 피질두께, 해마 부피 및 shape)를 측정하였다. 뇌 아밀로이드 침착의 양을 측정하기 위해 아밀로이드 페트를 활용하였고, 인지기능검사에서 기억력, 집행기능을 대표할 수 있는 조합점수를 도출하였다. 경로분석법으로 아밀로이드, 뇌혈관질환 병리, 뇌위축 및 인지기능저하 간의 관계를 분석하였다.

결과: 아밀로이드의 양은 해마 위축을 통해 기억력저하에 영향을 미쳤고, WMH는 전두엽의 위축을 통해 집행기능저하에

영향을 미쳤다. 아밀로이드의 양과 열공성 뇌경색은
해마/전두엽의 위축을 통하지 않은 직접경로를 통해 기억력 및 집행기능저하와 연관이 되어 있었다.
결론: 본 결과는 아밀로이드 및 뇌혈관질환 병리가 독립적으로 뇌위축 및 인지기능저하에 유의한 영향을 미치는 것을 확인하였고, 각각 고유힌 메커니즘을 통해 인지기능에 영향을 미치는 것을 확인하였다.

핵심되는 말 : 인지기능, 아밀로이드, 피츠버그 컴파운드 비, 뇌위축, 피질 두께, 해마, 경로분석, 뇌혈관질환, 자기공명영상, 알츠하이머 병, 경도인지장애

PUBLICATION LIST

1. Ye BS, Seo SW, Kim GH, Noh Y, Cho H, Yoon CW, et al. Amyloid burden, cerebrovascular disease, brain atrophy, and cognition in cognitively impaired patients. Alzheimers Dement 2014; Epub ahead of print.